scientific reports

Check for updates

OPEN

Structural controllability of general edge dynamics in complex network

Shaopeng Pang[1]✉, Yue Zhou[1], Xiang Ren[2] & Fangzhou Xu[3]

Dynamic processes that occur on the edge of complex networks are relevant to a variety of real-world systems, where states are defined on individual edges, and nodes are active components with information processing capabilities. In traditional studies of edge controllability, all adjacent edge states are assumed to be coupled. In this paper, we release this all-to-all coupling restriction and propose a general edge dynamics model. We give a theoretical framework to study the structural controllability of the general edge dynamics and find that the set of driver nodes for edge controllability is unique and determined by the local information of nodes. Applying our framework to a large number of model and real networks, we find that there exist lower and upper bounds of edge controllability, which are determined by the coupling density, where the coupling density is the proportion of adjacent edge states that are coupled. Then we investigate the proportion of effective coupling in edge controllability and find that homogeneous and relatively sparse networks have a higher proportion, and that the proportion is mainly determined by degree distribution. Finally, we analyze the role of edges in edge controllability and find that it is largely encoded by the coupling density and degree distribution, and are influenced by in- and out-degree correlation.

Complex networks containing interacting dynamic units are ubiquitous in social, financial and natural systems[1–3]. In recent years, the controllability of complex networks has received extensive attention and research[4–8]. Most studies of network controllability have focused on the nodal dynamics. However, the edge dynamics[9,10], which are relevant to various real-world systems, are also important in network science. It is suitable for modeling networks where states are defined on individual edges, and nodes are active components with information processing capabilities. A seminal work addressing edge controllability is presented by Nepusz et al.[9]. They introduced the switchboard dynamics (SBD) model to describe the edge dynamics and study its structural controllability. Much interest has been stimulated toward exploring the controllability properties of edge dynamics. Representative studies of edge dynamics include its controllable subspace[11], target control[12,13], controllability optimization[14], robustness[15], and applications in multi-agent systems[16–18].

Most of the existing work on the edge controllability describes the edge dynamics based on the SBD. The condition that the SBD requires all adjacent edge states to be coupled is too strong, which makes the SBD have certain limitations and cannot accurately describe various real-world systems. In this paper, we release this all-to-all coupling restriction and propose a general edge dynamics (GED) model that can describe the edge dynamics with arbitrary coupling relationships between edge states, which generalizes the SBD. For example, in the system with computers and routers, edges represent the physical connections such as fiber optics and cables. A node (i.e., a computer or router) continuously processes information received from some of its upstream neighbors and transmits it to some of its downstream neighbors. The information received and transmitted by a node can be represented by the states on its incoming and outgoing edges. The switching matrix in each node controls the dynamic process, and the elements in the switching matrix determine which upstream and downstream neighbors of a node to receive and transmit information. A social network can also be modeled as the GDE, in which people are nodes, the information transmitted between people are the edge states, and the switching matrix in each node controls the reception and transmission of information. The proposal of GED has caused a series of questions, such as the structural controllability of GED, the controllability characteristics, the role of coupling and the role of edges in the edge controllability, etc.

We study the structural controllability of edge dynamics based on the GED. Firstly, we give a theoretical framework to determine the minimum set of driver nodes and driven edges required to fully control the GED. We find that the set of driver nodes for edge controllability is unique and determined by the local information of nodes, which is fundamentally different from nodal controllability. Secondly, we find that the coupling density

[1]School of Information and Automation Engineering, Qilu University of Technology (Shandong Academy of Sciences), Jinan 250353, China. [2]Second Academy of China Aerospace Science and Industry Corporation, Beijing 100143, China. [3]International School for Optoelectronic Engineering, Qilu University of Technology (Shandong Academy of Sciences), Jinan 250353, China. ✉email: pang_shao_peng@163.com

among edge states plays an important role in edge controllability, where the coupling density is the proportion of adjacent edge states that are coupled. Specifically, there exist lower and upper bounds of edge controllability, which are determined by the coupling density. Meanwhile, there is a vast range between the controllability bounds, in which a broad spectrum of edge controllability can be achieved by adjusting the coupling density. We analyze empirical networks and propose theoretical formulations to demonstrate that the controllability bounds generally exist in the edge controllability of arbitrary networks. Thirdly, we investigate the proportion of effective coupling when controlling the GED. Simulation finds that homogeneous and relatively sparse networks have a higher proportion of effective coupling, and the proportion is mainly determined by the degree distribution. Finally, we analyze the role of edges in edge controllability by classifying each edge into one of three categories: critical, ordinary, and intermittent. We find that the proportions of the three kinds of edges are largely encoded by the coupling density and degree distribution, and are influenced by in- and out-degree correlation.

General edge dynamics

The SBD[9] provides a characterization of edge dynamics on a directed network $G(V, E)$. Let $\mathbf{y}_v^-$ and $\mathbf{y}_v^+$ represent the state vectors corresponding to the incoming and outgoing edge states of node v, respectively. The factor that can affect $\mathbf{y}_v^+$ is the vector $\mathbf{y}_v^-$, the damping vector $\boldsymbol{\tau}_v$, and the external input vector $\mathbf{u}_v$. Then the switchboard dynamics can be described as:

$$\dot{\mathbf{y}}_v^+ = S_v \mathbf{y}_v^- - \boldsymbol{\tau}_v \otimes \mathbf{y}_v^+ + \sigma_v \mathbf{u}_v, \tag{1}$$

where $S_v \in \mathbb{R}^{k_v^+ \times k_v^-}$ is the 'switching matrix'. The number of its row and column are equal to the out-degree k_v^+ and the in-degree k_v^- of node v, respectively. σ_v is one if node v is a driver node and is zero otherwise. $\otimes$ denotes the entry-wise product of the two vectors of the same size.

A linear time-invariant system can be established by reformulating Eq. (1) in terms of the edge state x_i, which is

$$\dot{\mathbf{x}} = (W - T)\mathbf{x} + H\mathbf{u}, \tag{2}$$

where $W \in \mathbb{R}^{M \times M}$ is the transpose of the adjacency matrix of the line graph $L(G)$ of G, in which w_{ij} is nonzero if and only if the head of edge j is the tail of edge i. For the line graph $L(G)$ converted from an original graph G, the nodes in $L(G)$ correspond to the edges in G, and an edge in $L(G)$ corresponds to a length-two directed path in G. $T \in \mathbb{R}^{M \times M}$ is a diagonal matrix whose diagonal elements correspond to the damping terms for each edge. Note that T can be ignored in the edge controllability[9,19]. $H \in \mathbb{R}^{M \times M}$ is a diagonal matrix where the ith diagonal element is σ_v if node v is the tail of edge i.

In the study of structural controllability[4,9], both the state and input matrices are structural matrices, where their elements are either fixed 0 or independent free parameters. A system is called structurally controllable if it is possible to fix the free parameters in the state and input matrices to certain values so that the obtained system is controllable in the usual sense, i.e., the generic rank of the controllability matrix

$$C = (H, WH, W^2 H, ..., W^{M-1} H), \tag{3}$$

has full rank $\mathrm{rank}_g(C) = M$, where the generic rank of a structural matrix is the maximal rank that the structural matrix achieves as a function of its free parameters.

However, the SBD requires all the elements in each switching matrix S_v are independent free parameters. The elements in S_v capture the coupling relationship between the incoming and outgoing edge states of nodes. The absence of 0 in S_v means that the incoming and outgoing edge states of each node are completely coupled. This restrictive conditions are too strong. We release this all-to-all coupling restriction and consider the GED, in which the elements in the switching matrix S_v are either fixed 0 or independent free parameters. The fundamental difference between SBD and GED is that GED allows 0 elements in the switching matrix. For example, An GED with 4 nodes and 5 edge states $\{x_1, x_2, x_3, x_4, x_5\}$ is shown in Fig. 1a. Its switching matrices $\{S_a, S_b, S_c, S_d\}$ contain either fixed 0 or independent free parameters.

Structural controllability of general edge dynamics

We are interested in configuring an appropriate input matrix H so that the GED is structurally controllable. The theory[9] no longer applies to the GED. We thus give a theoretical framework for the structural controllability of the GED, which is quantified based on the minimum number of driver nodes (i.e., the minimum number of nodes with $\sigma_v = 1$) and the minimum number of driven edges (i.e., the minimum number of non-zero columns of H) required to fully control the GED.

Equation (2) indicates that the GED of a digraph G is equivalent to the nodal dynamics of its trimmed line graph $L(G')$, where the nodes in $L(G')$ correspond to the edges in G, and an edge in $L(G')$ corresponds to an independent free parameter in the switching matrix of G. This equivalence shows that the GED of G and the nodal dynamics of $L(G')$ have the same state set and state matrix W. For example, as shown in Fig. 1a and c, the GED of a digraph G contains 5 edge states $\{x_1, x_2, x_3, x_4, x_5\}$ and 4 switching matrices $\{S_a, S_b, S_c, S_d\}$. Its trimmed line graph $L(G')$ is shown in Fig. 1b, where each independent free parameter in the switching matrix corresponds to a directed edge of $L(G')$. Taking S_a as an example, the independent free parameters in S_a correspond to edges e_{x_2, x_1} and e_{x_2, x_4} in $L(G')$, respectively.

We give the first method for determining the minimum number of driver nodes and driven edges required to fully control the GED. Firstly, applying the minimum input theorem[4] to the nodal dynamics of $L(G')$ gives us the bipartite graph $H(G)$. The maximum matching method[4] can determine the minimum unmatched nodes in $H(G)$, which correspond to the minimum driver nodes required to control the nodal dynamics of $L(G')$. For
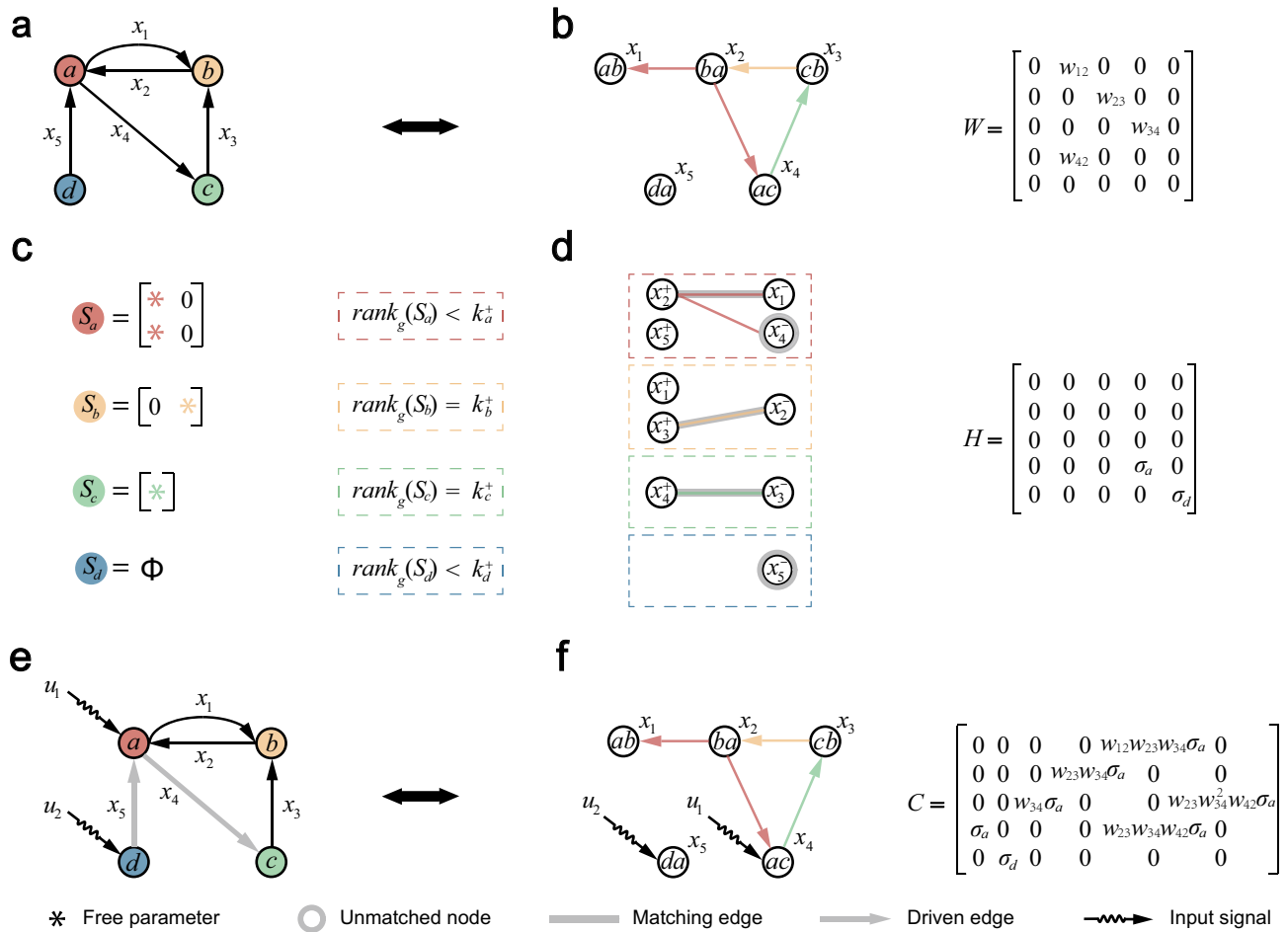
Figure 1. Structural controllability of general edge dynamics. (**a**) A directed network G with 4 nodes and 5 edge states $\{x_1, x_2, x_3, x_4, x_5\}$ in GED. (**b**) The trimmed line graph $L(G')$ of G. The colors of edges in $L(G')$ correspond to those of the nodes in (**a**). (**c**) The switching matrices $\{S_a, S_b, S_c, S_d\}$ in G. (**d**) The bipartite graph $H(G)$ of $L(G')$ with 4 matching blocks. (**e**) Driver nodes (v_a and v_d), driven edges (x_4 and x_5) and input signals (u_1 and u_2) for controlling the GED of G. (**f**) Driver nodes (x_4 and x_5) and input signals (u_1 and u_2) for controlling the nodal dynamics of $L(G')$.

example, the nodal dynamics of $L(G')$ and its bipartite graph $H(G)$ are shown in Fig. 1b and d, respectively. The unmatched nodes x_4 and x_5 in $H(G)$ is the driver nodes. How to controlling the nodal dynamics of $L(G')$ is shown in Fig. 1f. Secondly, the driver nodes in the nodal dynamics of $L(G')$ correspond one-to-one with the driven edges in the GED of G[9]. This allows us to determine the minimum number of driven edges needed to control the GED of G. For example, as shown in Fig. 1e and f, the driver nodes x_4 and x_5 in the nodal dynamics of $L(G')$ correspond to the driven edges x_4 and x_5 in the GED of G. Thirdly, the driver node required to control the GED of G is the starting node of the driven edge. As shown in Fig. 1e, the driver nodes are the starting nodes v_a and v_d of the driven edges. The generic rank of the controllability matrix has full rank $\text{rank}_g(C) = 5$, indicating that the GED of G is structurally controllable. In summary, we can determine the minimum number of driver nodes and driven edges required to control the GED with the help of minimum input theorem.

We further propose a framework to determine the minimum driver nodes and driven edges based on the local information of nodes, since the minimum input theorem is computationally complex and requires global information of network. Firstly, a bipartite graph $H(G)$ can be partitioned into N 'matching blocks' according to N switching matrices. The matching block corresponding to a switching matrix S_v contains the incoming edge states and outgoing edges edge states of the node v, where the incoming edge states and outgoing edges edge correspond to the left and right nodes of the matching block, respectively. Meanwhile the independent free parameters in S_v correspond one-to-one to the edges in the matching block. For example, as shown in Fig. 1c and d, taking S_a as an example, its matching block contains the edge states $\{x_2^+, x_5^+\}$ and $\{x_1^-, x_4^-\}$. The independent free parameters in S_a have a one-to-one correspondence with the edges in its matching block. Note that the incoming (outgoing) edge state of a node in GED is only coupled with the outgoing (incoming) edge state of this node, which means that the edges in the partitioned bipartite graph $H(G)$ only exist in each matching block, not between matching blocks. As shown in Fig. 1d, no edge spans any two matching blocks. This ensures that the maximum matching result of the partitioned bipartite graph $H(G)$ remains unchanged. Secondly, we prove that

the matching block of S_v contains unmatched nodes if and only if S_v has no full row rank, i.e., $\text{rank}_g(S_v) < k_v^+$. Meanwhile, the number of unmatched nodes in the matching block of S_v is equal to $k_v^+ - \text{rank}_g(S_v)$. The detailed proof process is in Supplementary Note 1. Thirdly, the driver nodes (unmatched nodes) in the nodal dynamics of $L(G')$ correspond one-to-one with the driven edges in the GED of G[9]. It can be deduced that, for the structural controllability of the GED of G, a node v is the driver node if $\text{rank}_g(S_v) < k_v^+$, and the number of driven edges in the outgoing edge set of the driver node is $k_v^+ - \text{rank}_g(S_v)$. As shown in Fig. 1c and d, taking S_a as an example, it is the driver node due to $\text{rank}_g(S_a) < k_a^+$. Meanwhile, the number of driven edges in the outgoing edge set of a is $k_a^+ - \text{rank}_g(S_a) = 1$.

Based on the above analysis, we present our major conclusions. The minimum number N_D of driver nodes required to control the GED is

$$N_\mathrm{D} = N_{(\text{rank}_g(S_v) < k_v^+)} + \sum_{i=1}^{N_\beta} \beta_i, \tag{4}$$

where $N_{(x)}$ is the number of nodes that satisfy the condition x. N_β is the number of connected components. $\beta_i = 1$ if the connected component is the full-rank component, and $\beta_i = 0$ otherwise, where the full-rank component is a strongly connected component with each node in it satisfies $k_v^- = k_v^+ = \text{rank}_g(S_v)$. Note that the accumulation term $\sum_{i=1}^{N_\beta} \beta_i$ is to ensure reachability. Specifically, we randomly select a node in each full-rank component as the driver node, and randomly select an outgoing edge of the driver node as the driven edge. Then the minimum number M_D of driven edges is

$$M_\mathrm{D} = \sum_{i=1}^{N} (k_i^+ - \text{rank}_g(S_i)) + \sum_{i=1}^{N_\beta} \beta_i. \tag{5}$$

The above formulas allow us to determine the minimum set of driver nodes and driven edges required to control the GED based on the local information of nodes. The detailed proof process is in Supplementary Note 1.

Controllability characteristics

We study the controllability characteristics of GED based on real and model networks. The controllability is quantitatively described by the proportion $n_D = N_D/N$ of driver nodes and the proportion $m_D = M_D/M$ of driven edges required for control. Since the switching matrix of GED contains 0 and independent free parameters, we introduce the coupling density $P \in [0, 1]$ to quantify the probability that an element in the switching matrix is an independent free parameter.

Figure 2a–f give the variation of n_D and m_D in Erdős-Rényi (ER), exponential (EX) and scale-free (SF) networks according to the coupling density P, the average degree $\langle k \rangle$ and the power exponent γ, respectively. An important finding is that there are upper and lower bounds on n_D and m_D. Specifically, when $P = 0$, there are no independent free parameters in the switching matrix, that is, there is no coupling between the incoming and outgoing edge states of any node, resulting in n_D and m_D reaching the upper bounds. Conversely, when $P = 1$, the incoming and outgoing edge states of each node are coupled, resulting in n_D and m_D reaching the lower bounds. Further, the gaps between the upper and lower bounds are very large, except for the case of small $\langle k \rangle$ and γ. Any values of n_D and m_D between bounds can be achieved by adjusting P. This demonstrates that the coupling density has a significant impact on the edge controllability. Another finding is that n_D of some ER networks shows a non-monotonic change with the increase of $\langle k \rangle$ in Fig. 2a, and larger value of P move the peak to the direction where $\langle k \rangle$ increases. The non-monotonic is caused by the different change rate of edges and couplings in these model networks with the change of $\langle k \rangle$. We provide a theoretical analysis of the non-monotonic. The details of the theoretical analysis are shown in model networks.

Figure 2g and j give n_D and m_D of the GED constructed from real network topologies. We find that the results for n_D and m_D vary greatly with the coupling density P, but do not exceed the upper bound (when $P = 0$) and lower bound (when $P = 1$). Another important factor affecting n_D and m_D is the degree distribution. Therefore, we apply a degree-preserving randomization (rand-degree)[4], which keeps the in- and out-degrees of each node unchanged but reconnects the nodes randomly. As shown in Fig. 2h and k, this procedure does not alter N_D and M_D significantly. Equations (4) and (5) show that N_D and M_D are determined by the local network information (i.e., in- and out-degrees of each node and coupling density) and the full-rank component. The degree-preserving randomization can keep the local network information unchanged, but it can hardly generate new full-rank components. Therefore, N_D and M_D of a degree-preserving randomization are very close to those of its original network. This indicates that n_D and m_D are determined mainly by the coupling density and degree distribution. Furthermore, we bring the coupling density and the degree distribution of real networks into our theoretical formulas to give analytical predictions of n_D and m_D. As shown in Fig. 2i and l, for most real networks, a good agreement is obtained between the analytical predictions and the real results. The values of n_D and m_D of the real network are shown in Table 1. See Supplementary Note 3 for the details of theoretical predictions for real networks.

In summary, we find that the coupling density has a significant impact on the edge controllability, leading to the controllability bounds being pervasive in both model and real networks. We can estimate the edge controllability of the network based on the coupling density and degree distribution.
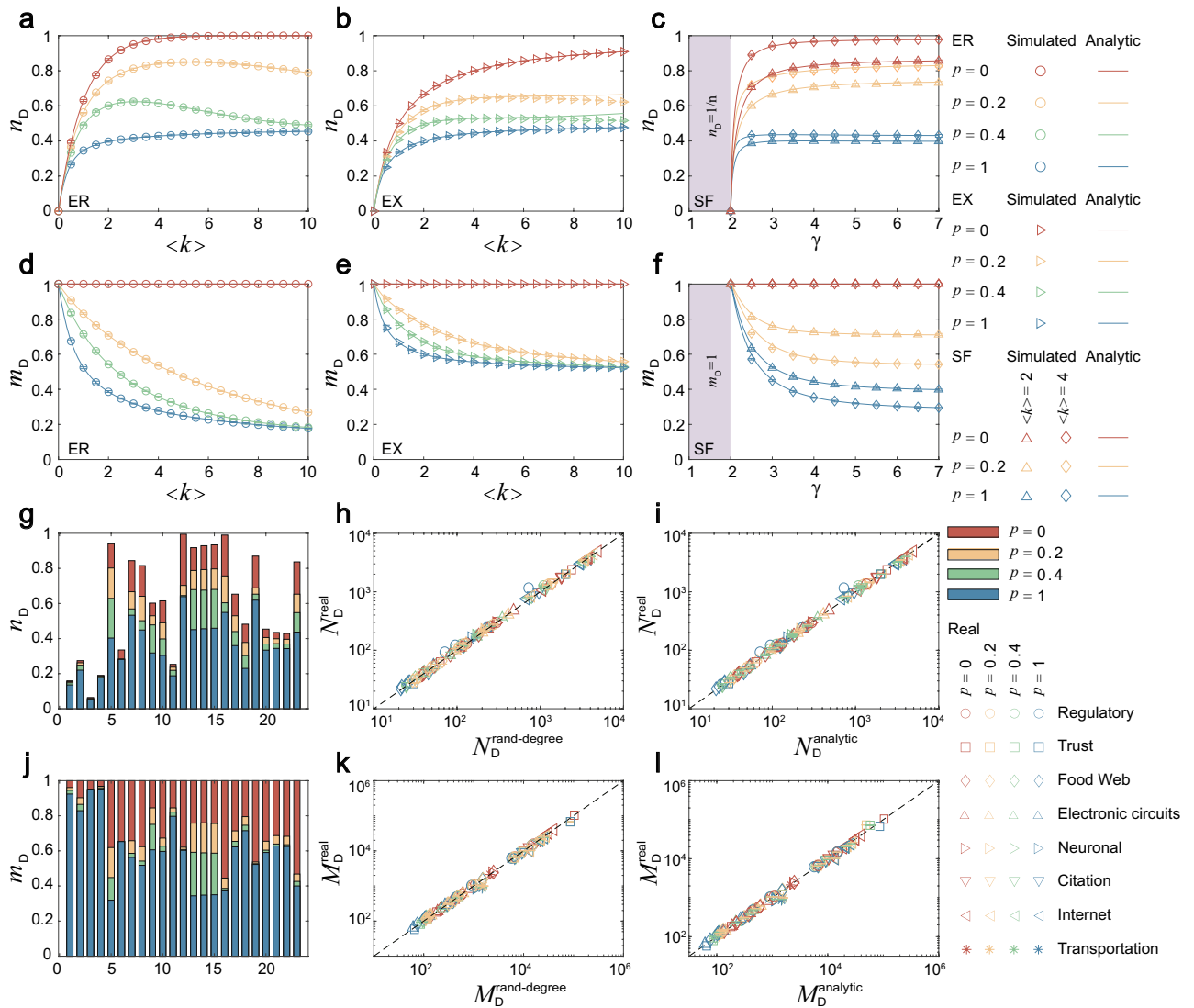
Figure 2. Controllability characteristics. The variation of n_D and m_D in (**a**, **d**) ER networks, (**b**, **e**) EX networks, and (**c**, **f**) SF networks as the function of the coupling density P, the average degree $\langle k \rangle$ and the power exponent γ, respectively. The results of (**g**) n_D and (**j**) m_D in real networks with $P = 0$, $P = 0.2$, $P = 0.4$, and $P = 1$, respectively. Numbers refer to the network indices in Table 1. The results of (**h**) $N_D^{\text{rand-degree}}$ and (**k**) $M_D^{\text{rand-degree}}$ obtained from the degree-preserving randomized version of the real networks, compared with the real results, respectively. The theoretical predictions of (**i**) N_D^{analytic} and (**l**) M_D^{analytic} compared with the real results, respectively. All the numerical results are obtained by averaging over 100 independent network realizations.

The role of coupling

We study the role of coupling (i.e., independent free parameter) on the edge controllability. Firstly, we gradually increase the coupling density P until the number M_D of driven edges required to control the GED reaches the lower bound. Let the coupling density at this time be P_O, as shown in Fig. 3a, we find that the P_O of most real networks is not high. This shows that most of the coupling are ineffective, that is, their absence does not affect the edge controllability.

This inspires us to study the proportion of effective coupling. Specifically, for a node v, we delete the independent free parameters in its switching matrix S_v one by one under the premise that the number of driven edges in its outgoing edge set remains unchanged. We find that the minimum number of independent free parameters is equal to the generic rank of the switching matrix. Therefore, the proportion of effective coupling is

$$P_E = \frac{1}{N} \sum_{i=1}^{N} \text{rank}_g(S_i)/(k_i^+ k_i^- P), \tag{6}$$

where $k_i^+ k_i^- P$ is the number of independent free parameters in the switching matrix of a node, and $\text{rank}_g(S_i)$ is the minimum number of independent free parameters that keeps the number of driven edges in the outgoing
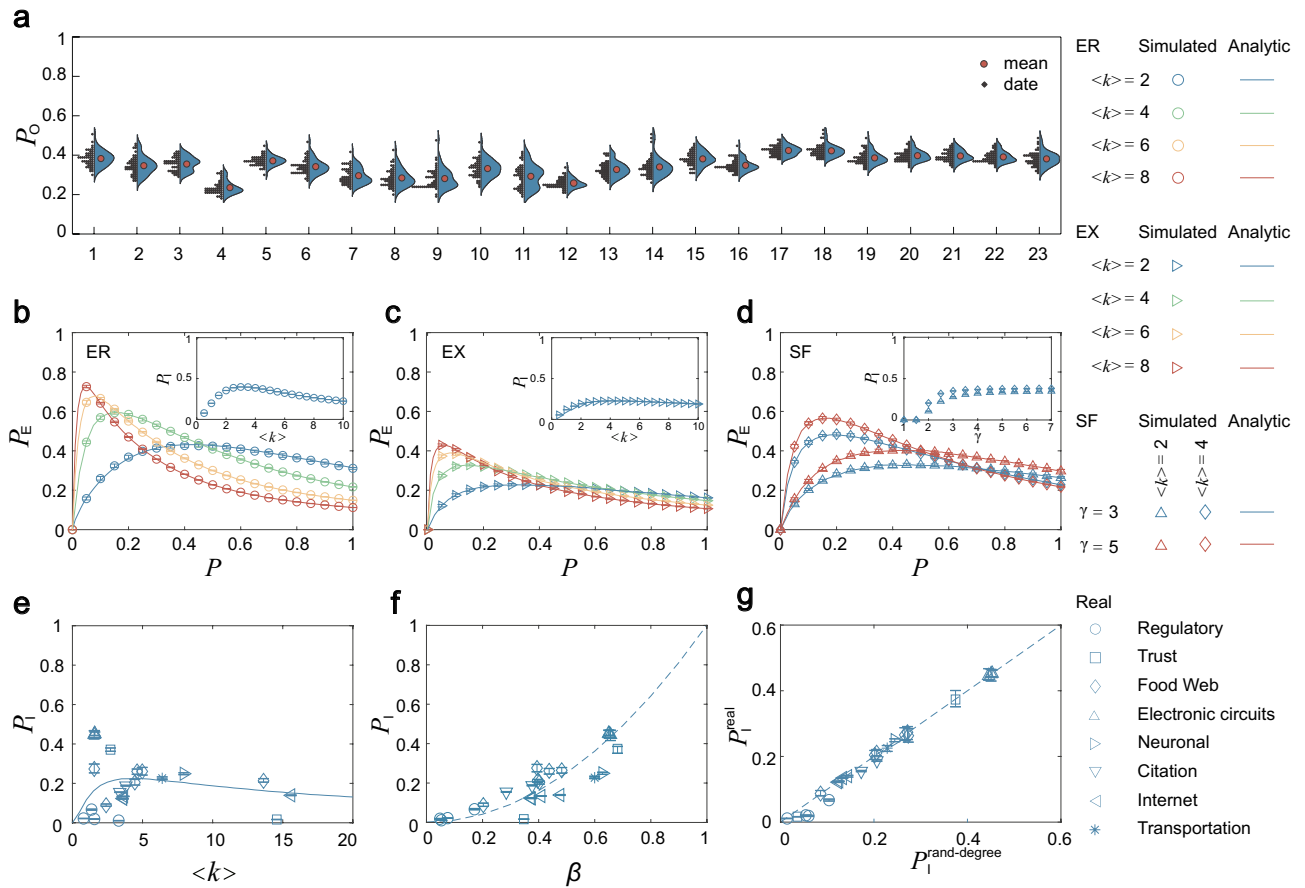
Figure 3. The role of coupling. (**a**) The half violin plot of P_O for real networks. The proportion P_E of effective coupling and its trapezoidal numerical integration P_I in (**b**) ER networks, (**c**) EX networks, and (**d**) SF networks as the function of the coupling density P, the average degree $\langle k \rangle$ and the power exponent γ, respectively. (**e**) The integration P_I of real networks as the function of $\langle k \rangle$. (**f**) The integration P_I of real networks as the function of the correlation parameter β. (**g**) The integration $P_I^{rand-degree}$ obtained from the degree-preserving randomized version of the real networks, compared with P_I^{real}.

edge set of this node unchanged. Figure 3b–d give the variation of P_E in ER, EX and SF networks according to the coupling density P, the average degree $\langle k \rangle$ and the power exponent γ, respectively. An important finding is that P_E and P are not positively correlated, as P_E decreases with increasing P when P is large enough. This confirms the conclusion that P_O is not high in real networks. Another interesting phenomenon is that P_E shows a distinct peak for a specific value of P. Both the location and the height of the peak mainly depend on $\langle k \rangle$, and larger value of $\langle k \rangle$ moves the peak to the direction where P decreases.

To further study the effect of network topology on P_E, we give the trapezoidal numerical integral of P_E in the interval $[0, 1]$, denoted as P_I. The integral operation allows P_I to be independent of P and is only relevant to the network topology. As shown in the panels in Fig. 3b–d, we find that homogeneous (i.e., big γ) and relatively sparse (i.e., small $\langle k \rangle$) networks have the highest P_I. Then we analyze the effect of network topology on P_I based on real networks. On the one hand, we give the dependence of P_I of real networks on $\langle k \rangle$. As shown in Fig. 3e, P_I of relatively sparser real networks is higher, which confirms the results based on model networks. On the other hand, we give the dependence of P_I of real networks on the correlation parameter[6], i.e., $\beta = 1 - \frac{1}{2M} \sum_i |k_i^+ - k_i^-|$. The parameter $\beta \in [0, 1]$ captures the in- and out-degree correlation of a network. For example, $\beta = 1$ indicates the perfect positive correlation between in- and out-degrees of nodes, i.e., $k_v^+ = k_v^-$ for each node. As shown in Fig. 3f, there is a basic positive correlation between P_I and β, which further states that the homogeneous networks have higher P_I. To analyze the dependence of P_I in the real network, we apply degree-preserving randomization. As shown in Fig. 3g, this procedure does not alter P_I significantly. This indicates that P_I is determined mainly by the degree distribution. In other words, P_I is determined mainly by the number of incoming and outgoing edges of each node and is independent of where those edges point. The values of P_O and P_I of the real network are shown in Table 1.

In summary, we find that most of coupling are ineffective in edge controllability. Homogeneous and relatively sparse networks have a higher proportion of effective coupling. The proportion of effective coupling is mainly determined by the degree distribution.
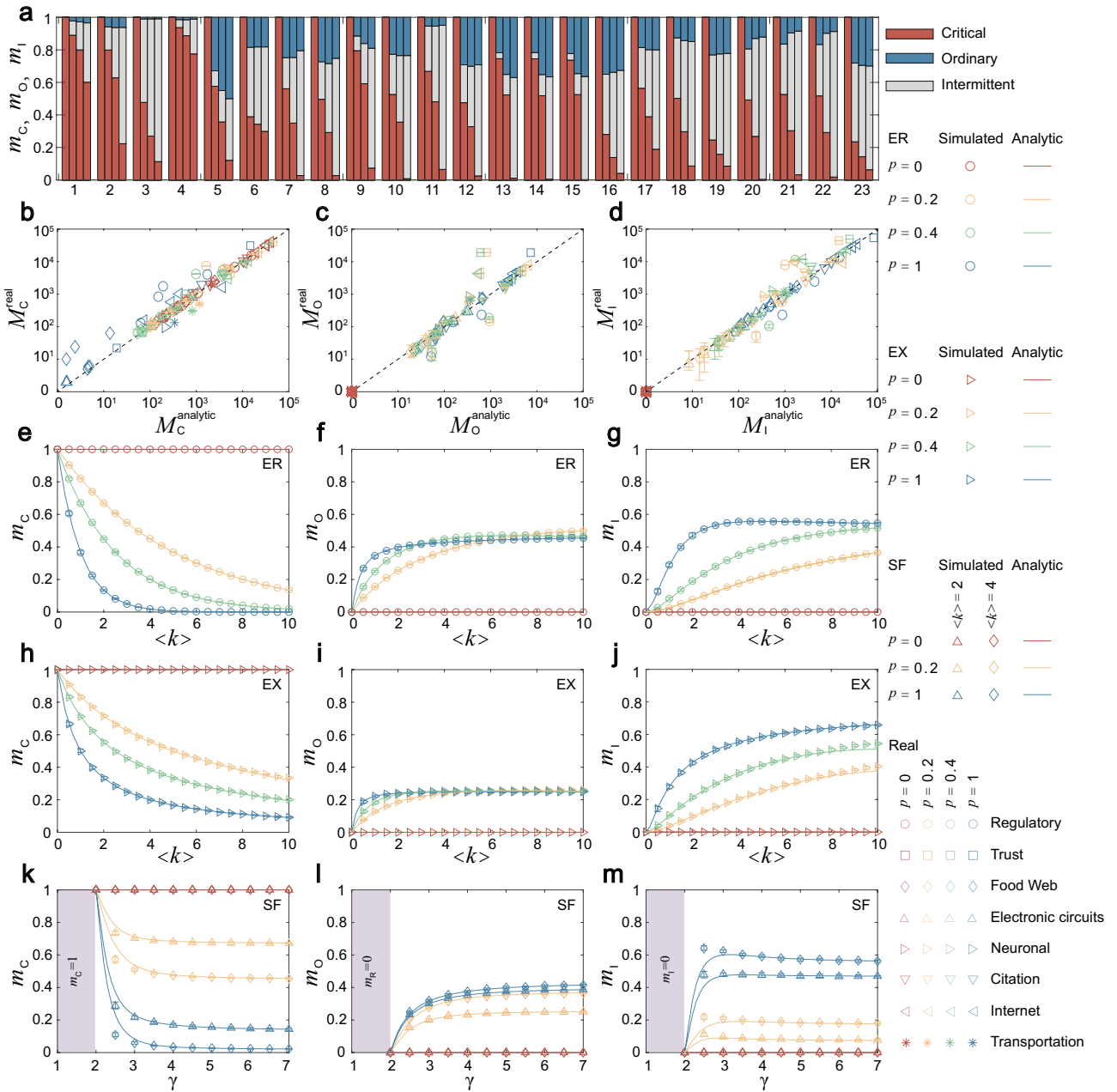
Figure 4. The Role of Edges. (**a**) The proportion of critical m_C, ordinary m_O, and intermittent m_I edges in each real network with the coupling density $P = 0$, $P = 0.2$, $P = 0.4$, and $P = 1$, respectively. The proportion (**b**) M_C^{analytic}, (**c**) M_O^{analytic}, and (**d**) M_I^{analytic} obtained by theoretical prediction, compared with the real results. The variation of m_C, m_O, and m_I in (**e–g**) ER networks, (**h–j**) EX networks, and (**k–m**) SF networks as the function of the coupling density P, the average degree $\langle k \rangle$ and the power exponent γ, respectively.

The role of edges

We explore the role of edges in edge controllability by classifying each edge into one of three categories[20]: critical, ordinary, and intermittent. Specifically, critical means that an edge must be the driven edge; ordinary means that it is not the driven edge and intermittent means that it belongs to the set of driven edges with a certain probability. We neglect the possible presence of full-rank component, which is uncommon in directed networks and has little effect on the number M_D of driven edges. Then the category of an edge depends solely on the switching matrix of its source node. Specifically, the number of driven edges in the set of outgoing edges of a driver node v is $k_v^+ - \text{rank}_g(S_v)$. Therefore, the judgment methods of the three kinds of edges are as follows:

(1) An edge is critical if it corresponds to an all-zero row in the switching matrix of its source node. In particular, an edge is critical if its source node satisfies $k_v^+ > k_v^- = 0$.

Type	No.	Name	N	M	n_D^L	n_D^U	m_D^L	P_O	P_I	$m_C^{P=1}$	$m_O^{P=1}$	$m_I^{P=1}$
Regulatory	1	Ownership − USCorp[21]	8497	6726	0.136	0.159	0.924	0.384	0.022	0.601	0.034	0.365
	2	TRN − EC − 2 [22]	423	578	0.220	0.274	0.829	0.348	0.068	0.223	0.062	0.715
	3	TRN − Yeast − 1[23]	4684	15451	0.052	0.064	0.947	0.356	0.011	0.113	0.009	0.878
	4	TRN − Yeast − 2[22]	688	1079	0.177	0.190	0.952	0.236	0.019	0.775	0.011	0.214
Trust	5	prison inmate[24,25]	67	182	0.403	0.940	0.319	0.372	0.374	0.121	0.500	0.379
	6	WikiVote[26]	7115	103689	0.281	0.335	0.653	0.342	0.017	0.299	0.182	0.519
Foodweb	7	St.Marks[27]	45	224	0.533	0.844	0.563	0.296	0.263	0.027	0.205	0.768
	8	Seagrass[28]	49	226	0.449	0.816	0.518	0.286	0.262	0.027	0.252	0.721
	9	grassland[29]	88	137	0.318	0.602	0.606	0.282	0.278	0.073	0.190	0.737
	10	Ythan[29]	135	601	0.304	0.615	0.597	0.332	0.205	0.008	0.235	0.757
	11	Silwood[30]	154	370	0.188	0.253	0.797	0.293	0.087	0.065	0.049	0.886
	12	Little Rock[31]	183	2494	0.639	0.995	0.603	0.258	0.210	0.025	0.292	0.683
Electronic circuits	13	S208a[22]	122	189	0.451	0.918	0.344	0.329	0.446	0.011	0.370	0.619
	14	S420a[22]	252	399	0.456	0.929	0.348	0.341	0.446	0.005	0.366	0.629
	15	S838a[22]	512	819	0.459	0.934	0.350	0.382	0.452	0.002	0.364	0.634
Neorunal	16	C.elegans[32]	297	2359	0.549	0.990	0.374	0.349	0.249	0.041	0.326	0.633
Citation	17	Scimet[33]	2729	1041	0.360	0.653	0.623	0.424	0.188	0.189	0.200	0.611
	18	Kohonen[34]	3772	12731	0.230	0.482	0.715	0.424	0.155	0.086	0.149	0.765
Internet	19	Political blogs [35]	1224	19090	0.619	0.870	0.523	0.388	0.140	0.085	0.222	0.693
	20	p2p − 1[36]	10876	39994	0.334	0.454	0.591	0.398	0.134	0.004	0.121	0.875
	21	p2p − 2[36]	8846	31839	0.344	0.435	0.628	0.397	0.124	0.032	0.085	0.883
	22	p2p − 3[36]	8717	31525	0.343	0.429	0.625	0.391	0.130	0.018	0.087	0.895
Transportation	23	USair97[37]	332	2126	0.437	0.837	0.400	0.382	0.252	0.063	0.299	0.638

Table 1. Structural controllability of general edge dynamics in real network. For each network, we obtain its type, number, name, number N of nodes, number M of edges, the lower bounds $\left(n_D^L \text{ and } m_D^L\right)$, the upper bound $\left(n_D^U \text{ and } m_D^U\right)$, P_O, P_I and the proportions of the three kinds of edge $\left(m_C^{P=1}, m_O^{P=1}, m_I^{P=1}\right)$. Note that, when $P=0$, we have $m_D^U=1, m_C^{P=0}=1, m_O^{P=0}=0, m_I^{P=0}=0$.

(2) An edge is ordinary if $\mathrm{rank}_g(S_v) > \mathrm{rank}_g(S'_v)$, where S_v is the switching matrix of the source node v of the edge, and S'_v is the switching matrix of v after deleting the non-zero row corresponding to the edge.

(3) An edge is intermittent if $\mathrm{rank}_g(S_v) = \mathrm{rank}_g(S'_v)$.

We employ the real and model networks to substantiate the edge categories and offer analytical results. The proportions of critical, ordinary and intermittent edges in each real network with the coupling density $P = 0$, $P = 0.2$, $P = 0.4$, and $P = 1$ are shown in Fig. 4a. A notable finding is that as P increases, the proportion of critical edges in each real network is drastically reduced and replaced by ordinary and intermittent edges. The reason is that as P increases, the all-zero rows in the switching matrix gradually sparse. This facilitates that most real networks are dominated by ordinary and intermittent edges when P is large enough. Note that the existence of a few star-shaped giants in the regulatory networks (No. 1 and 4 in Table 1) is responsible for their large number of critical edges.

The way of identifying edges can be used to derive analytical formulas for the expected fraction of three edge categories in real and model networks (see Supplementary Note 2 and 3 for the detailed procedures). As shown in Fig. 4b–d, a good agreement is obtained between the theoretical predictions and the real results. This shows that the proportions of three kinds of edges can be predicted by considering the coupling density and degree distribution. Note that the reason why the theoretical predictions deviate slightly from the real results is that the theoretical predictions are performed by assuming that in- and out-degrees of nodes have no correlation in real networks. Then we give the simulation and analytical results of model networks. One of the main findings is that P has a significant impact on the proportion of the three kinds of edges, especially in dense and homogeneous networks. For ER networks in Fig. 4e–g, we find that at low $\langle k \rangle$, the networks are dominated by critical edges. The reason is that abundant nodes without an incoming edge exist in the networks. As the network grows, the fraction of ordinary and intermittent edges increases rapidly. As shown in Fig. 4h–j, the trends of the curves in EX networks are very similar to those provided by ER networks. But the fraction of ordinary edges is smaller, counterbalanced by a greater proportion of critical and intermittent edges. Figure 4k–m give the variation of three kinds of edges in SF networks with γ. We find that heterogeneous (small γ) networks are dominated by critical edges. However, when P is large enough, the homogeneous network contains very few critical edges, replaced by ordinary and intermittent edges. The values of m_C, m_O and m_I of the real network are shown in Table 1.

In conclusion, we find that the proportions of three kinds of edges are to a great extent encoded by the coupling density and the degree distribution, and are affected by the in- and out-degree correlation. When the coupling density is large enough, dense and homogeneous networks have lower proportions of critical edges, replaced by ordinary and intermittent edges.

Conclusion

Most existing research on edge controllability is based on the SBD. However, the SBD requires all adjacent edge states to be coupled. This restrictive conditions are too strong. In this paper, we release this all-to-all coupling restriction and propose the GED, which can describe the edge dynamics with arbitrary coupling relationships between edge states. We give a theoretical framework to study the structural controllability of GED. An important finding is that the set of driver nodes for edge controllability is unique and determined by the local information of nodes, where the local information of a node includes in-degree, out-degree and the generic rank of its switching matrix. Then we find that the coupling density among edge states plays an important role, leading to the lower and upper bounds of edge controllability. At the same time, we can estimate the edge controllability of an arbitrary network based on its coupling density and degree distribution. Furthermore, we investigate the role of coupling and edges in edge controllability.

Our findings raise many open questions. For example, is it possible to achieve partial control of a subset of edge states in GED from a minimal number of driver nodes? Could a method be developed to implement target control of GED? How to optimize edge controllability with small perturbations of coupling and network structure? What is the energy cost of controlling GED?

Data availability

The data generated and analysed during the current study are available from the corresponding author on reasonable request.

References

1. Newman, M. E. J. Networks: An introduction (2010).
2. Barabási, A. L. Linked: The new science of networks (2003).
3. Albert, R. & Barabási, A. L. Statistical mechanics of complex networks. *Rev. Mod. Phys.* **74**, 47. https://doi.org/10.1103/RevModPhys.74.47 (2002).
4. Liu, Y. Y., Slotine, J. J. & Barabási, A. L. Controllability of complex networks. *Nature* **473**, 167–173. https://doi.org/10.1038/nature10011 (2011).
5. Yuan, Z., Zhao, C., Di, Z., Wang, W. X. & Lai, Y. C. Exact controllability of complex networks. *Nat. Commun.* **4**, 1–9. https://doi.org/10.1038/ncomms3447 (2013).
6. Gao, J., Liu, Y. Y., D'souza, R. M. & Barabási, A. L. Target control of complex networks. *Nat. Commun.* **5**, 1–8. https://doi.org/10.1038/ncomms6415 (2014).
7. Yan, G. *et al.* Spectrum of controlling and observing complex networks. *Nat. Phys.* **11**, 779–786. https://doi.org/10.1038/nphys3422 (2015).
8. Liu, Y. Y. & Barabási, A. L. Control principles of complex systems. *Rev. Mod. Phys.* **88**, 035006. https://doi.org/10.1103/RevModPhys.88.035006 (2016).
9. Nepusz, T. & Vicsek, T. Controlling edge dynamics in complex networks. *Nat. Phys.* **8**, 568–573. https://doi.org/10.1038/Nphys2327 (2012).
10. Slotine, J. J. & Liu, Y. Y. The missing link. *Nat. Phys.* **8**, 512–513. https://doi.org/10.1038/nphys2342 (2012).
11. Pang, S. P. & Hao, F. Controllable subspace of edge dynamics in complex networks. *Phys. A* **481**, 209–223. https://doi.org/10.1016/j.physa.2017.04.034 (2017).
12. Pang, S. P. & Hao, F. Target control of edge dynamics in complex networks. *Phys. A* **512**, 14–26. https://doi.org/10.1016/j.physa.2018.08.011 (2018).
13. Lu, F., Yang, K. & Qian, Y. Target control based on edge dynamics in complex networks. *Sci. Rep.* **10**, 1–12. https://doi.org/10.1038/s41598-020-66524-6 (2020).
14. Pang, S. P. & Hao, F. Optimizing controllability of edge dynamics in complex networks by perturbing network structure. *Phys. A* **470**, 217–227. https://doi.org/10.1016/j.physa.2016.12.001 (2017).
15. Pang, S. P., Hao, F. & Wang, W. X. Robustness of controlling edge dynamics in complex networks against node failure. *Phys. Rev. E* **94**, 052310. https://doi.org/10.1103/PhysRevE.94.052310 (2016).
16. Zheng, X., Ji, Z. & Yu, H. Controllability of edge dynamics on directed multi-agent systems. In *2018 Chinese Control And Decision Conference (CCDC)* 2489–2493. https://doi.org/10.1109/ccdc.2018.8407543 (2018).
17. Nguyen, D. H. Edge dynamics based distributed formation controller design for unmanned vehicle groups. In *2019 IEEE Vehicle Power and Propulsion Conference (VPPC)* 1–5. https://doi.org/10.1109/VPPC46532.2019.8952226 (2019).
18. Shi, C. X. & Yang, G. H. Robust consensus control for a class of multi-agent systems via distributed PID algorithm and weighted edge dynamics. *Appl. Math. Comput.* **316**, 73–88. https://doi.org/10.1016/j.amc.2017.07.069 (2018).
19. Pang, S. P., Wang, W. X., Hao, F. & Lai, Y. C. Universal framework for edge controllability of complex networks. *Sci. Rep.* **7**, 1–12. https://doi.org/10.1038/s41598-017-04463-5 (2017).
20. Li, C. & Pang, S. The role of individual edges in edge controllability of complex networks. *IEEE Access* **8**, 63559–63566. https://doi.org/10.1109/ACCESS.2020.2984358 (2020).
21. Kim Norlen, G. L., Gebbie, M. & Chuang, J. Eva: Extraction, visualization and analysis of the telecommunications and media ownership network. In *International Telecommunications Society 14th Biennial Conference (ITS2002), Seoul, Korea* (2002).
22. Milo, R. *et al.* Network motifs: Simple building blocks of complex networks. *Science* **298**, 824–827. https://doi.org/10.1126/science.298.5594.824 (2002).
23. Balaji, S., Babu, M. M., Iyer, L. M., Luscombe, N. M. & Aravind, L. Comprehensive analysis of combinatorial regulation using the transcriptional regulatory network of yeast. *J. Mol. Biol.* **360**, 213–227. https://doi.org/10.1016/j.jmb.2006.04.029 (2006).
24. Milo, R. *et al.* Superfamilies of evolved and designed networks. *Science* **303**, 1538–1542. https://doi.org/10.1126/science.1089167 (2004).
25. Van Duijn, M. A., Zeggelink, E. P., Huisman, M., Stokman, F. N. & Wasseur, F. W. Evolution of sociology freshmen into a friendship network. *J. Math. Sociol.* **27**, 153–191. https://doi.org/10.1080/00222500305889 (2003).
26. http://snap.stanford.edu/data/wiki-Vote.html.
27. Baird, D., Luczkovich, J. & Christian, R. R. Assessment of spatial and temporal variability in ecosystem attributes of the St Marks National Wildlife Refuge, Apalachee Bay, Florida. *Estuar. Coast. Shelf Sci.* **47**, 329–349. https://doi.org/10.1006/ecss.1998.0360 (1998).

28. Christian, R. R. & Luczkovich, J. J. Organizing and understanding a winter's seagrass foodweb network through effective trophic levels. *Ecol. Model.* **117**, 99–124. https://doi.org/10.1016/S0304-3800(99)00022-8 (1999).
29. Dunne, J. A., Williams, R. J. & Martinez, N. D. Food-web structure and network theory: The role of connectance and size. *Proc. Natl. Acad. Sci.* **99**, 12917–12922. https://doi.org/10.1073/pnas.192407699 (2002).
30. Memmott, J., Martinez, N. & Cohen, J. Predators, parasitoids and pathogens: Species richness, trophic generality and body sizes in a natural food web. *J. Anim. Ecol.* **69**, 1–15. https://doi.org/10.1046/j.1365-2656.2000.00367.x (2000).
31. Martinez, N. D. Artifacts or attributes? Effects of resolution on the little rock lake food web. *Ecol. Monogr.* **61**, 367–392. https://doi.org/10.2307/2937047 (1991).
32. Watts, D. J. & Strogatz, S. H. Collective dynamics of 'small-world' networks. *Nature* **393**, 440–442. https://doi.org/10.1038/30918 (1998).
33. http://vlado.fmf.uni-lj.si/pub/networks/data/cite/default.htm.
34. http://www.cise.ufl.edu/research/sparse/matrices/Pajek/Kohonen.html.
35. Adamic, L. A. & Glance, N. The political blogosphere and the 2004 us election: Divided they blog. In *Proceedings of the 3rd International Workshop on Link Discovery* 36–43. https://doi.org/10.1145/1134271.1134277 (2005).
36. Leskovec, J., Kleinberg, J. & Faloutsos, C. Graph evolution: Densification and shrinking diameters. *ACM Trans. Knowl. Discov. Data (TKDD)* https://doi.org/10.1145/1217299.1217301 *(2007)*.
37. http://2018.icbeb.org/Challenge.html.

Acknowledgements

Author contributions

S.P. was responsible for the overall idea and revising the paper. Y.Z. contributed mainly to data processing, experimental design, and writing the paper. X.R. was responsible for reviewing the paper. F.X. made contributions to review the paper and revise of the manuscript during manuscript revision.

Competing interests

The authors declare no competing interests.

Additional information

Supplementary Information The online version contains supplementary material available at https://doi.org/10.1038/s41598-023-30554-7.

Correspondence and requests for materials should be addressed to S.P.

Reprints and permissions information is available at www.nature.com/reprints.

Publisher's note Springer Nature remains neutral with regard to jurisdictional claims in published maps and institutional affiliations.